IEEE Access
Multidisciplinary | Rapid Review | Open Access Journal

Received April 20, 2019, accepted May 14, 2019, date of publication May 27, 2019, date of current version June 24, 2019.

*Digital Object Identifier 10.1109/ACCESS.2019.2919274*

# Experimental Study of LoRa Modulation Immunity to Doppler Effect in CubeSat Radio Communications

**ALEXANDER A. DOROSHKIN[1], ALEXANDER M. ZADOROZHNY[1], OLEG N. KUS[2], VITALIY YU. PROKOPYEV[1], AND YURI M. PROKOPYEV[1]**

[1]Division for Atmospheric Research, Novosibirsk State University, 630090 Novosibirsk, Russia
[2]OKB Fifth Generation Ltd., 630090 Novosibirsk, Russia

Corresponding author: Alexander M. Zadorozhny (zadorozh@phys.nsu.ru)

This work was supported by the Ministry of Science and Higher Education of the Russian Federation under Project RFMEFI57517X0154.

**ABSTRACT** Currently, LoRa technology is one of the most promising technologies in satellite Internet of Things. Particularly those based on satellite constellations in low Earth orbit, including the CubeSat nanosatellite constellations. However, the LoRa specification does not contain clear criteria for the applicability of the LoRa modulation under strong Doppler effect conditions caused by the very high speed of satellites. This is especially true in the case of the dynamic Doppler effect when the Doppler frequency shift changes rapidly with time. This paper presents the results of laboratory testing and outdoor experiments conducted to determine the feasibility of the LoRa modulation in CubeSat radio communication systems. Additionally, possible restrictions associated with the Doppler effect were explored. The experiments showed that the LoRa modulation has very high immunity to the Doppler effect. This immunity allows for the use of LoRa modulation in satellite radio communications in orbits above 550 km without any restrictions associated with the Doppler effect. In lower orbits, the dynamic Doppler effect leads to the destruction of the satellite-to-Earth radio channel when using the LoRa modulation mode with a maximum spreading factor of $SF = 12$. This destruction occurs when the satellite is flying directly above the ground station, resulting in reduced duration of the radio communication session. The reduction in the duration of a communication session increases with decreasing orbit altitude and reaches about one minute in an ultra-low orbit 200 km high.

**INDEX TERMS** CubeSat radio communication, Doppler effect, laboratory testing, LoRa modulation, multipath propagation, outdoor experiments.

## I. INTRODUCTION

LoRa is a proprietary modulation scheme [1] used in infrastructure solutions for the Internet of Things (IoT) [2], [3]. The LoRa modulation is based on the chirp spread spectrum (CSS) technique where the data is encoded by a wideband chirp signal in which the frequency linearly increases or decreases with time [4], [5]. The CSS modulation technique is preferred for use in IoT wireless networks due to its relatively low transmission power requirements and inherent robustness against channel degradation mechanisms such as multipath, fading and Doppler effect. LoRa can improve receiver sensitivity by more than 20 dB compared to conventional frequency shift keying (FSK). This enables long communication ranges or the reduction of transmission power, thus lowering transmitter energy consumption [4].

Low transmission power enabled by LoRa modulation and its robustness against the Doppler effect are important properties not only for IoT technologies, but also for possible applications in radio communication systems of very small satellites (nanosatellites) of CubeSat class. Initially conceived in 1999 as an educational tool, CubeSat has become a standard low-cost platform for space and technology research [6], [7]. The low energy budget of CubeSat necessitates the use of low consumption onboard systems including the radio communication system. A very high

The associate editor coordinating the review of this manuscript and approving it for publication was Mohammad Tariqul Islam.

relative velocity (about 8 km/s) between a satellite moving in Earth orbit and a ground station requires a very high robustness of the satellite-to-Earth radio channel against the Doppler effect. Currently, LoRa is considered one of the most promising technologies for use in satellite IoT projects based on satellite constellations in low Earth orbit (LEO) [8], [9], including the CubeSat constellation [10]. However, the LoRa modulation specification does not contain clear criteria regarding applicability when the receiver rapidly moves relative to the transmitter, especially when the Doppler shift changes rapidly with time. The latter takes place when a satellite is flying over a ground station.

Two practical experiments were carried out in [11] to assess the practical capabilities and constraints of the LoRa technology under Doppler frequency shift. In the first experiment, the LoRa end device was mounted to a lathe, installed in a laboratory environment, which was used to generate different angular velocities for the end device. In the second experiment, the LoRa end device was mounted to a car that was driven via a motorway passing the LoRa IoT gateway. In contrast with declared robustness of the LoRa modulation against the Doppler effect, both experiments clearly showed that the LoRa communication performance deteriorates when relative speed between the end device and the gateway exceeds 40 km/h. This value is about three orders of magnitude lower than the speed of the LEO satellite.

A similar result in an experiment with a LoRa transceiver installed in a moving car was obtained in [12]: even with a small vehicle speed of about 8 km/h, the packet loss rate increased significantly.

A recent paper [13] also described an experiment with a LoRa transmitter moving in a car past a LoRa receiver. The speed of the car during the experiment ranged from 50 km/h to 80 km/h. In contrast to [11] and [12], the results of [13] did not show a noticeable influence of the Doppler effect on the packet loss rate even at a maximum speed of 80 km/h.

In [14], we performed laboratory experiments to test the LoRa modulation immunity to Doppler effect under conditions corresponding to satellite-to-Earth radio communication. A software-defined radio (SDR) transmitter was used in the experiments to synthesize a radio frequency signal with the LoRa modulation, taking into account the Doppler shift corresponding to the satellite-to-Earth radio channel. The synthesized signal was fed via cable to a standard LoRa receiver using a Semtech SX1278 chip [15]. We carried out experiments for several LoRa modulation parameters. The results of experiments showed high immunity of the radio channel using LoRa modulation to the Doppler effect at cosmic velocities up to a few tens of kilometers per second.

Thus, on the one hand, there is experimental data confirming the high robustness of the LoRa modulation to the Doppler effect [13], [14]. On the other hand, there is experimental data showing that the Doppler effect begins to have a significant impact on the LoRa radio channel at receiver speeds relative to the transmitter from about 8 km/h to 40 km/h [11], [12].

The objectives of this work are to give a convincing explanation regarding the contradictions between the works mentioned, and to demonstrate the possibilities and possible restrictions on the use of LoRA modulation in space applications under very strong Doppler shift conditions. To do this, we performed additional laboratory and outdoor field experiments. In the laboratory, in addition to the previously performed measurements [14], we tested the LoRa modulation immunity to the Doppler effect for the same LoRa parameters that were used in [11]. We also checked, in the laboratory, the behavior of the LoRa receiver as it moves assuming multipath propagation of the LoRa signal, emulating the experimental conditions in [11] and [12]. Then, we conducted outdoor experiments, with the LoRa receiver installed in a car, similarly to [11] and [12], but only with strict enforcement of line-of-sight conditions between the moving receiver and transmitter.

In this paper, we present the results of these new experiments, which are related to our previous work [14], in order to provide convincing evidence of the very high immunity of the LoRa modulation to the Doppler effect at cosmic speeds of the receiver relative to the transmitter. The paper is organized as follows. Section 2 of the paper describes the laboratory experiments. Outdoor measurements are presented in Section 3. A summary of the results and conclusions are given in Section 4.

## II. LABORATORY TESTING

### A. LABORATORY EQUIPMENT

A software-defined radio transmitter and a standard LoRa receiver were used for laboratory testing and experimental studies of the radio link utilizing the LoRa modulation. Using an SDR transmitter allows not only the synthesis of a pure RF signal with the LoRa modulation. Additionally, the SDR permits introduction of various random and deterministic interferences into the synthesized signal, including the frequency shift caused by the Doppler effect. We used a modular NI PXIe-5672 radio frequency vector signal generator by National Instruments Corporation [16] as a SDR transmitter, and a LoRa transceiver based on the SX1278 chip by the Semtech Corporation [15] as a receiver and demodulator. The modular NI PXIe-5672 generator was embedded into a NI PXIe-1062Q chassis operated by an NI PXIe-8130 controller. The LoRa transceiver was also controlled by the NI PXIe-8310 via USB interface. The output of the NI PXIe-5672 generator was connected through a coaxial cable to the input of the LoRa receiver. This excludes any possible impact from uncontrolled environmental conditions to affect the results of the investigations. A photo of the laboratory setup for testing LoRa modulation is shown in Fig. 1.

The LoRa signal is synthesized by means of the software, developed for this research in LabVIEW using the NI-RFSG driver software. The NI PXIe-5672 generator synthesizes the LoRa radio signal taking into account the Doppler shift and the LoRa receiver receives, demodulates and analyzes this signal. The analysis of the quality of the received signal and

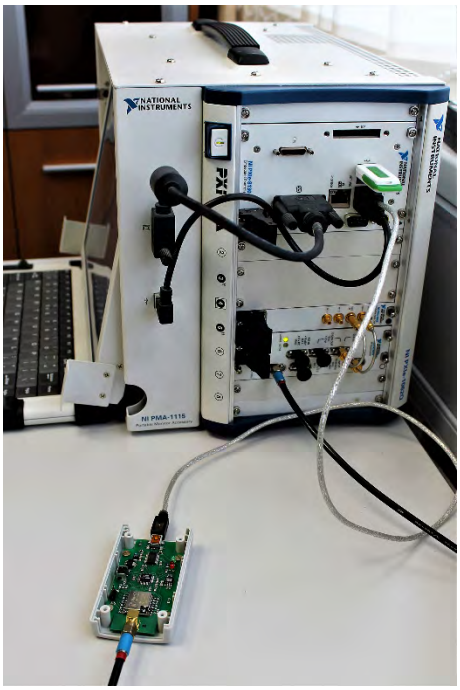

**FIGURE 1.** Laboratory setup for testing LoRa modulation.

the data packages contained therein are carried out using data from the internal registers of the receiver. For the experiments performed, we synthesized the LoRa radio signal with a carrier frequency of 434 MHz.

### B. SATELLITE RADIO COMMUNICATION

Answering whether is it possible to apply the LoRa modulation for satellite radio communications is one of the goals of the performed laboratory experiments. Therefore, a main part of the experiments has been carried out emulating a radio link between a ground station and satellite flying in low Earth orbit over the station with a speed of about 8 km/s.

In order to synthesize a high-frequency radio signal with LoRa modulation propagating in a radio link between the satellite and the ground station, it is necessary to model the time varying Doppler frequency shift as the satellite flies over the station. If transmitter emits a radio signal with a frequency $F_0$, due to the Doppler effect, the receiver will get a signal with frequency

$$F = \frac{1}{1 + \frac{v}{c}\cos\beta} \cdot F_0 \tag{1}$$

where $v$ is the satellite velocity, $c$ is the light speed, $\beta$ is the angle between the satellite velocity vector and the direction to the ground station. Then the relative Doppler frequency shift $\delta F$ is defined by:

$$\delta F = \frac{F - F_0}{F_0} = \frac{1}{1 + \frac{v}{c} \cdot \cos(\beta)} - 1. \tag{2}$$

For a satellite moving on a circular orbit of height $H$ and a ground station situated in a plain of the orbit, the relative

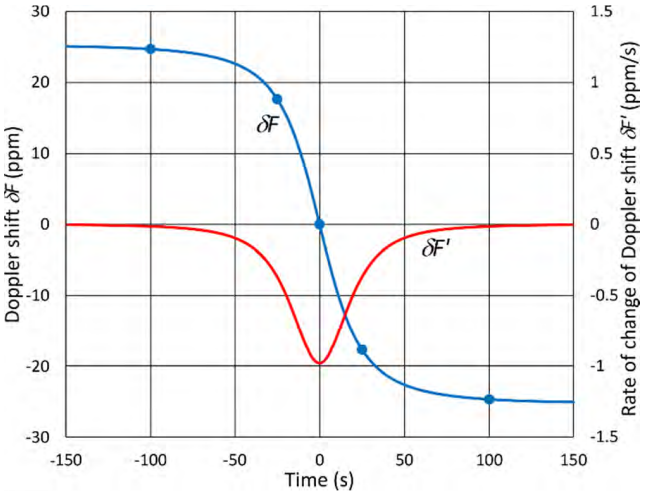


**FIGURE 2.** The relative Doppler shift and the rate of its change during the passage of the satellite at an altitude of 200 km above the ground station. The satellite is at its zenith above the ground station at time $t = 0$. Bold points indicate the times at which laboratory measurements have been performed.

Doppler shift $\delta F$ is defined by equation [14]:

$$\delta F = \frac{1}{1 + \frac{1}{c} \cdot \sqrt{\frac{g \cdot R}{1 + \frac{H}{R}}} \cdot \frac{\sin(\varphi)}{\sqrt{\left(1 + \frac{H}{R}\right)^2 - 2 \cdot \left(1 + \frac{H}{R}\right) \cdot \cos(\varphi) + 1}}} - 1 \tag{3}$$

where

$$\varphi = \frac{\sqrt{g/R}}{(1 + H/R)^{3/2}} \cdot t. \tag{4}$$

Here $R$ is the radius of the Earth, $g$ is the gravitational acceleration on the surface of the Earth, and it is assumed that time $t$ is zero when the satellite is at its zenith above the ground station.

The speed of a satellite in a circular orbit, which is defined by expression

$$v = \sqrt{\frac{g \cdot R}{1 + H/R}}, \tag{5}$$

increases with decreasing altitude of the orbit. As a result the Doppler effect is most pronounced when the satellite moves at low altitudes. Therefore, we investigated the impact of the Doppler effect on the LoRa radio channel for a satellite moving in an extremely low circular orbit with an altitude of 200 km at a speed of about 7.9 km/s. The relative Doppler shift $\delta F$ in ppm units (parts per million), calculated from (3) for this orbit, and its time derivative $\delta F'$ are shown in Fig. 2. It should be noted that the ultralow Earth orbit with a height of 200 km is not a working orbit for nanosatellites, since the lifetime of CubeSat satellites in this orbit is only a few days due to atmospheric drag [17].

In our experiments, the NI PXIe-5672 vector signal generator synthesized a radio frequency LoRa signal with a Doppler shift that varies with time as shown in Fig. 2. That is, the synthesized RF signal takes into account the dynamic

**TABLE 1. LoRa modulation parameters selected for the laboratory measurements.**

| Set No. | *SF* | *BW*, kHz | LoRa payload size, byte | Transmission time of a LoRa packet, s |
|---|---|---|---|---|
| 1 | 7 | 125 | 255 | 0.55 |
| 2 | 11 | 250 | 255 | 2.5 |
| 3 | 12 | 125 | 59 | 2.7 |

Doppler effect, i.e. the time varying Doppler shift. The rate of change of the Doppler shift $\delta F'$ reaches its maximum when the satellite is at the zenith above the ground station, and the Doppler shift is zero ($t = 0$ in Fig. 2). Bold points in Fig. 2 correspond to specific portions of the satellite trajectory in the context of radio conditions where conditions are among the most extreme. In particular these points are at the maximum static Doppler effect when the satellite is near the horizon, at the maximum dynamic Doppler effect when the satellite is at its zenith ($t = 0$), and at intermediate positions where there is a large Doppler shift with a high rate of change. Testing the LoRa radio link was carried out for these specific segments of the satellite trajectory.

The main parameters, which determine the data bit rate for the LoRa modulation, are the spreading factor (*SF*) and the spread spectrum modulation bandwidth (*BW*). The SX1278 transceiver used in the experiments offers *BW* options ranging from 7.8 kHz to 500 kHz with *SF* ranging from 6 to 12. The immunity of the radio link with the LoRa modulation to the Doppler effect was tested with three sets of LoRa parameters. These are given in Table 1. In the first set, the transmission time of a LoRa packet is close to the lowest possible value for maximum payload size. In the second and third sets, it is close to the maximum possible one. The LoRa modulation also includes a variable error correction scheme [4]. In the experiments, we used a coding rate of 4/5, which ensures the detection of errors in the communication channel, but does not correct them.

The synthesized LoRa signal with a carrier frequency of 434 MHz and power of about −100 dBm was fed via a cable to the input of the SX1278 transceiver operating as a receiver and a demodulator. The criterion of communication quality was the lossless reception of all transmitted data packets received with the correct checksum. The performed measurements showed excellent quality of the satellite LoRa communication channel despite the Doppler effect for spreading factor $SF = 7$ and 11 (sets of LoRa parameters No. 1 and 2 in Table 1) for all specific trajectory segments shown in Fig. 2. We did not detect transmitted data losses in these experiments. It should be noted that for the dynamic Doppler effect the stability of the LoRa radio link under the considered conditions is ensured only if a parameter of the LoRa modulation *LowDataRateOptimize* is activated. The third bit of the *RegModemConfig3* register of the SX1278 transceiver activates this parameter [15].

As for the spreading factor $SF = 12$ (Set 3 in Table 1), radio communication was stable only on the trajectory segment near $t = 100$ s, i.e. only in the conditions of the static Doppler effect.

Thus, we determined the degree of immunity of the LoRa modulation to the Doppler effect for typical conditions of communication between a ground station and a satellite in a low Earth orbit. Then we conducted measurements to determine the maximum possible Doppler shift, up to which the LoRa modulation still works, as well as the maximum allowable rate of change of the Doppler shift. The first case is associated with the static Doppler effect, and the second with the dynamic Doppler effect. When testing the static Doppler effect, we initially found the approximate Doppler shift values, for each set of LoRa parameters from Table 1, at which data loss begins to occur, and then carried out detailed measurements in the vicinity of these values. When measuring, we changed the Doppler frequency shift with a constant step. Initially, we chose the $\delta F$ change step of 44.268 Hz (0.102 ppm) so that it was less than the SX1278 transceiver frequency synthesizer step (61 Hz) [15] and not a multiple of it. With this step, measurements were made for the spreading factor $SF = 11$ (Set 2 in Table 1). However, in order to reduce the measurement time, the step was doubled, and in the measurement for sets 1 and 3 it was equal to 88.536 Hz (0.204 ppm). We transmitted 50 data packets at each step, and the successfully received packets were counted. The *LowDataRateOptimize* LoRa modulation parameter was activated during the experiments. The measurement results are shown in Fig. 3.

Fig. 3a shows that the LoRa radio channel with $SF = 7$ operates stably without losing data up to $\delta F \approx 71$ppm. With large Doppler shifts, data packets begin to be lost. With $\delta F$ exceeding about 72 ppm, the probability of successful transmission of a data packet drops to zero. For the spreading factor $SF = 11$ and $SF = 12$, the picture is different (see Figures 3b and 3c). After a certain value of the Doppler shift is exceeded, the probability of successful data packet transmission changes unsystematically from 0 to 100%. We cannot definitively explain the reason for this behavior. Most likely, this is due to the specific implementation of the SX1278 transceiver and the algorithm for digital frequency synthesis and frequency tuning.

Similarly, we determined the maximum allowable rates of change of the Doppler frequency shift. The maximum rate occurs when the frequency shift changes rapidly near its zero value. Fig. 4 shows the measurement results obtained with the LoRa modulation parameter *LowDataRateOptimize* activated. The results of measurements with the spreading factor $SF = 7$, performed with the non-activated parameter, are shown in Fig. 5. We see that the maximum allowable rate of change of the Doppler frequency shift decreases sharply with an increase in the spreading factor *SF* from 7 to 11 and 12. Deactivating *LowDataRateOptimize* parameter drastically worsens the stability of the LoRa radio channel in dynamic Doppler conditions. For $SF = 7$, deactivating this parameter reduces the maximum allowable rate of change of the Doppler frequency shift by almost two orders of magnitude from about 150 ppm/s to 2.1 ppm/s (see Fig. 4a and Fig. 5).

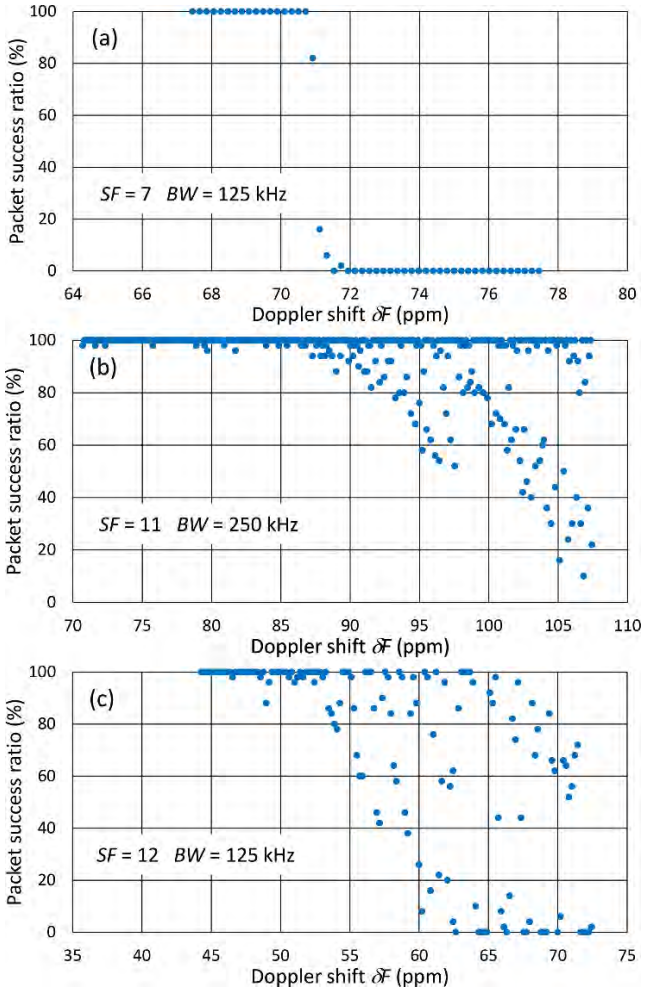


**FIGURE 3.** Packet success ratio at different Doppler shift: (a) $SF = 7$ and $BW = 125$ kHz, (b) $SF = 11$ and $BW = 250$ kHz, (c) $SF = 12$ and $BW = 125$ kHz.

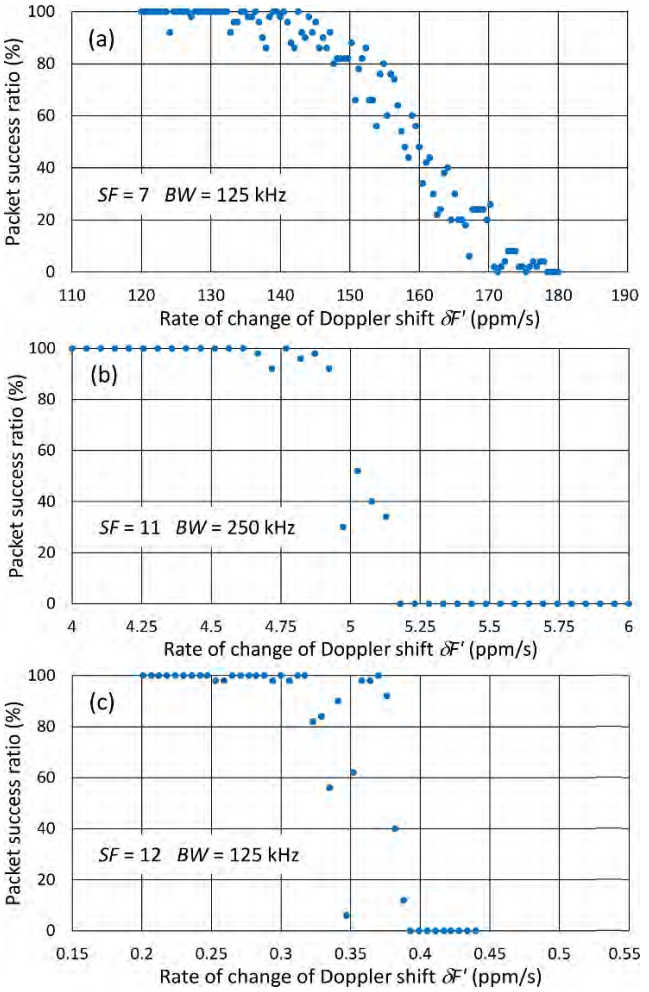


**FIGURE 4.** Packet success ratio at different rate of change of the Doppler frequency shift: (a) $SF = 7$ and $BW = 125$ kHz, (b) $SF = 11$ and $BW = 250$ kHz, (c) $SF = 12$ and $BW = 125$ kHz.

**TABLE 2.** Results of testing a LoRa radio channel for resistance to the Doppler effect.

| $SF$ | $BW$, kHz | Static Doppler effect ($\delta F' = 0$) | | Dynamic Doppler effect ($\delta F = 0$) |
|---|---|---|---|---|
| | | $\delta F_{\max}$, ppm | $v_{r,\max}$, km/s | $\delta F'_{\max}$, ppm/s |
| 7 | 125 | 71 | 21.3 | 150 (2.1[a]) |
| 11 | 250 | 94.5 | 28.3 | 4.94 |
| 12 | 125 | 55 | 16.5 | 0.33 |

[a]With non-activated LoRa modulation parameter *LowDataRateOptimize*.

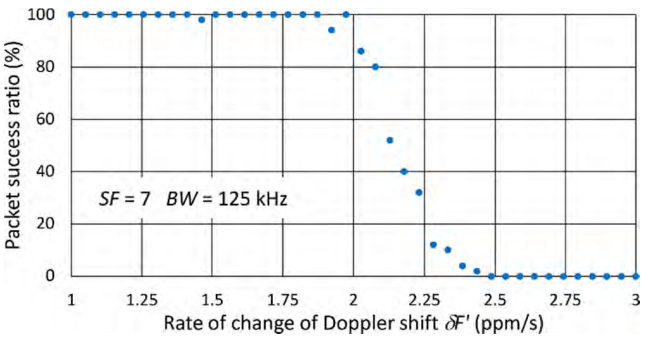


**FIGURE 5.** Packet success ratio at different rate of change of the Doppler frequency shift with non-activated LoRa modulation parameter ***LowDataRateOptimize***.

The results of laboratory testing a LoRa radio channel for resistance to the Doppler effect are summarized in Table 2. Here, $\delta F_{\max}$ and $\delta F'_{\max}$ are the maximum values of the Doppler shift and the rate of its change, up to which the probability of successful transmission of a data packet exceeds 70% (see Fig. 3, Fig. 4 and Fig. 5). The corresponding values of the maximum allowable receiver speed relative to the transmitter $v_r = v \cdot \cos(\beta)$ are also shown here. We see high reliability of the LoRa modulation in the presence of a static Doppler shift up to 55–94.5 ppm, which corresponds to a receiver speed of about 16.5–28.3 km/s relative to the transmitter. The robustness against the dynamic Doppler effect holds for rates of change of Doppler frequency shift up to 0.33–150 ppm/s, depending on the LoRa parameters $SF$ and $BW$.

In the case of the static Doppler effect, the measured maximum tolerated values of the relative Doppler frequency shift $\delta F_{\max}$ are 71 ppm, 94.5 ppm and 55 ppm for $SF = 7$, 11 and

12. These values coincide rather well with the specification of the LoRa SX1278 transceiver [15]. The specification of the tolerated frequency offset between the transmitter and the receiver for the same modulation modes and the carrier frequency of 434 MHz are 73, 100 and 50 ppm, respectively. As for the dynamic Doppler effect, the specification of the LoRa SX1278 transceiver does not contain any restrictions on the rate of change of Doppler frequency shift $\delta F'_{\max}$.

The results show that for spreading factors $SF \leq 11$ the obtained values of $\delta F_{\max}$ and $\delta F'_{\max}$ (Table 2) are several times higher than the Doppler shift and its rate of change in a satellite-to-Earth radio channel (Fig. 2). This means that we have a significant margin of immunity of the LoRa modulation to the Doppler effect when using LoRa modulation with $SF \leq 11$ in satellite communication systems. In the case $SF = 12$, which ensures maximum sensitivity of the LoRa receiver with a minimum bandwidth of the communication channel, the situation becomes more complicated. At $SF = 12$, there is also a significant margin of immunity of the LoRa modulation to the static Doppler effect, sufficient to apply the LoRa modulation in satellite radio communications. However, the LoRa modulation becomes unworkable due to the strong dynamic Doppler effect in ultra-low Earth orbit 200 km high as the satellite flies over a ground station. The expected rate of change of the Doppler shift in this case is about 1 ppm/s (see Fig. 2), which is about three times its maximum allowable value $\delta F'_{\max} = 0.33$ ppm/s, obtained in the experiments (Table 2). This means when using $SF = 12$ for satellite radio communication with a ground station, the duration of a communication session decreases in this orbit by about one minute (see Fig. 2) due to loss of communication during satellite flight directly above the ground station. As follows from (5), as the orbit height increases, the satellite speed decreases, thus the time interval during which the LoRa modulation does not work decreases. Using (3), we obtained that for circular orbits with a height of more than 550 km, the rate of change of the Doppler frequency shift $\delta F'_{\max}$ never exceeds 0.33 ppm/s. That is, in these orbits, the LoRa modulation with $SF = 12$ kHz is suitable for use in satellite-to-ground radio communications without any restrictions associated with the Doppler effect.

A characteristic feature of satellite-to-Earth radio communications is line-of-sight radio wave propagation. The high robustness of the LoRa modulation against the Doppler effect, which was found in our laboratory experiments, refers precisely to such conditions. In the next section, we will show how the stability of the LoRa radio channel is compromised under signal multipath propagation conditions in the presence of the Doppler effect.

### C. MULTIPATH LORA SIGNAL PROPAGATION

In the studies outlined in [11], two experiments with LoRa end devices were carried out. In one experiment the LoRa devices were installed on a lathe and in the other on a car and both were carried out in real urban conditions. In contrast with our laboratory results, which correspond to line-of-sight conditions, both experiments clearly showed that the LoRa communication performance deteriorates when the relative speed between the end device and the gateway exceeds 40 km/h. In all cases, the received LoRa signal was significantly higher than the receiver sensitivity. A similar result was obtained in [12].

**TABLE 3. Parameters of the four multipath components selected for the LoRa testing under conditions of multipath signal propagation.**

| Path No. | Relative amplitude, $A_i$ | Angle $\beta_i$, degree | Phase $\varphi_i$, degree |
|---|---|---|---|
| 1 | 1 | 0 | 0 |
| 2 | 0.5 | 90 | 180 |
| 3 | 0.2 | 60 | 180 |
| 4 | 0.1 | 75.5 | 180 |

LoRa radio signal propagation in an urban environment is subject to multipath wave propagation caused by reflection from buildings and other terrestrial objects. In this case, the different Doppler shifts of each multipath component reaching the moving receiving antenna from different directions will lead to multipath fading effects [18]. A detailed analysis of the fading effects due to Doppler spread is not the task of this paper. In this section, we present only the results of laboratory experiments that show how multipath wave propagation can destroy LoRa radio communication, even if the LoRa signal is significantly higher than the receiver sensitivity.

Let us consider a receiver moving relative to a stationary transmitter with a velocity $v$. Suppose that there are four paths of the LoRa signal propagation from the transmitter to the receiver. Relative amplitudes $A_i$, angles between the velocity vector of the receiver and the direction of arrival of the signal $\beta_i$, and phases $\varphi_i$, of the four multipath components that were selected for the laboratory testing are shown in Table 3.

According to (2), each multipath component has its own Doppler shift. The summation of the four signals with different frequencies leads to a signal at the receiver input with a time-varying amplitude. Using the NI PXIe-5672 vector signal generator, we synthesized this complete RF LoRa signal, which arrived at the receiver input from the transmitter via the four paths for different receiver speeds. We used $SF = 12$ and $BW = 125$ kHz in this experiment. Temporal changes in the amplitude of the signal at the receiver input are shown in Fig. 6 for $v = 40$ km/h. At other speeds, the form of the amplitude temporal variations remains unchanged, only the time scale changes. The temporal changes in the amplitude of the signal at the receiver input are shown in Fig. 6 at a critical average signal level, below which transmitted data begins to be lost. The red line in Fig. 6 shows the LoRa receiver sensitivity in the modulation mode used.

The results of the experiment can be explained as follows. When the receiver speed increases, the fade time of the signal at the receiver input decreases, and the speed at which the signal amplitude decreases during fading increases. After reaching a certain critical value of the signal fade rate, the receiver apparently does not have time to track the rapid changes in

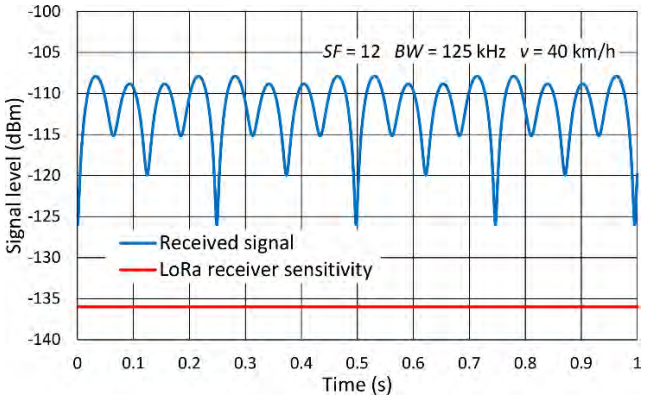


**FIGURE 6.** The temporal changes in the amplitude of the LoRa signal at the receiver input in the conditions of four-path propagation and the Doppler effect. The amplitude changes are shown at a critical signal level, below which the transmitted data begins to lose at a receiver speed of 40 km/h.

the signal amplitude. Thus, the connection is broken and data loss occurs even when the input signal amplitude exceeds the receiver sensitivity.

The results of our laboratory experiment with multipath propagation of a LoRa radio signal are in very good agreement with the results of field experiments in natural urban conditions [11]. In both kinds of experiments, field and laboratory, data loss is observed in the LoRa radio channel when the receiver moves while experiencing multipath propagation of the signal. This loss occurs even if the amplitude of the input signal significantly exceeds the sensitivity of the receiver. This allows us to conclude that the deterioration of the LoRa radio channel when the receiver moves in an urban environment at a speed of more than 40 km/h, found in [11], is not the result of the pure Doppler effect, but the result of the combination of multipath and Doppler effects. This means that the results of [11] are not applicable to satellite LoRa radio communications, since in this case there is no multipath signal propagation.

## III. OUTDOOR EXPERIMENTS

To confirm the conclusion of the previous section about the inapplicability of the results of [11] and [12] to satellite radio communications, we conducted our own outdoor experiments with a LoRa receiver installed in a moving car. The experiments were carried out similarly to [11] and [12], but we ensured line-of-sight conditions between the moving receiver and transmitter. This line-of-sight condition excludes multipath propagation of the signal.

In our outdoor experiments, we used two SX1278 transceivers installed inside two cars. One car remained motionless during the experiments, and the second drove past the first one on the highway. During the experiments, single-board computers Raspberry Pi 2 Model B [19] controlled the LoRa SX1278 transceivers via USB interface. Time synchronization and determination of the transceiver coordinates and speeds were carried out using GLONASS/GPS navigation receivers. Transceiver antennas were located on the roofs of the cars (Fig. 7).

**FIGURE 7.** The 434 MHz antenna mounted on the roof of the car during the outdoor experiments.

**TABLE 4.** LoRa modulation parameters selected for the outdoor experiments.

| No. | *SF* | *BW*, kHz | LoRa payload size, byte | Transmission time of a LoRa packet, s | LoRa receiver sensitivity, dBm |
|---|---|---|---|---|---|
| 1 | 8 | 250 | 255 | 0.46 | -123 |
| 2 | 8 | 500 | 255 | 0.23 | -119 |
| 3 | 12 | 62.5 | 21 | 2.97 | -139 |

The LoRa modulation parameters for which the outdoor experiments were performed are shown in Table 4. The experiments used a 4/5 coding rate, which ensures the detection of errors in the communication channel, but does not correct them. In addition, each transmitted data packet contained a unique serial number. Data loss was detected by checksum and the absence of packets with the transmitted unique serial numbers in the received data.

Fig. 8 shows a Google map of the area where the outdoor experiments were conducted. The territory mainly contains agricultural land. In the northeast direction from the highway, there is practically no vegetation. A forest protection belt is located along the southwest border of the highway. The stationary car with a LoRa transmitter was located near the crossroad on the side of the highway. The forest protection belt and the turn of the highway, approximately 850 meters from the location of the transmitter, limit the line-of-sight in the northwest direction. In the opposite direction, the line-of-sight conditions are lost about 600 meters from the transmitter due to the terrain profile, a rather sharp drop in the height of the Earth's surface relative to the location of the transmitter. The second car with the LoRa receiver started driving along the highway to the northwest from the location of the transmitter to turn 1, and then to the southeast to turn 2 or 3

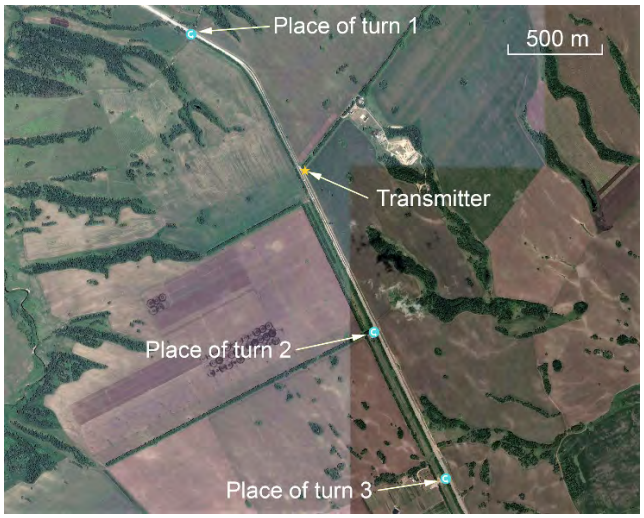


**FIGURE 8.** Google map of the area where the outdoor experiments were conducted.

(see Fig. 8). In each experiment with the LoRa modulation parameters from Table 4, the car with the receiver made two complete rounds on the highway between the place of turn 1 and the place of turn 2 (or 3). The maximum speed of the car reached was about 120 km/h. The results of the outdoor experiments are shown in Fig. 9, Fig. 10, and Fig. 11.

Fig. 9 shows the results of experiment No. 1 (in accordance with Table 4), performed with the LoRa modulation parameters $SF = 8$ and $BW = 250$ kHz. The distribution of successfully received (blue dots) and lost (red dots) data packets in the phase path of the receiver is shown in Fig. 9a. As in the laboratory experiments, here the relative speed $v_r = v \cdot \cos(\beta)$ is the speed of the moving receiver relative to the fixed transmitter, $v$ is the speed of the car with the receiver, and $\beta$ is the angle between the speed of the car and the direction to the transmitter. The relative velocity $v_r > 0$ when the receiver approaches the transmitter, and $v_r < 0$ when it moves away from the transmitter. The positive distance between the receiver and the transmitter corresponds to the position of the receiver on the highway in the northwest direction from the transmitter, and the negative distance – in the southeast direction. The area in which the line-of-sight conditions are met is highlighted in green. Figures 9b and 9c show the signal levels and the signal-to-noise ratio at the receiver input measured by the built-in means of the SX1278 transceiver.

In total, during experiment No. 1, 638 data packets were transmitted, of which seven packets were lost. As can be seen from Fig. 9a, all packet loss occurred outside the line-of-sight. Fig. 9b shows that the signal at the receiver input dropped to −126 dBm in areas where data packet losses were observed. The signal-to-noise ratio in these areas decreased to about −8.5 dB (Fig. 9c). Since the sensitivity of the LoRa receiver with the modulation parameters used in this experiment is −123 dBm (see Table 4), the loss of data packets outside the line-of-sight is quite understandable in this case. Recall that the line-of-sight in our experiments is limited in the southeast

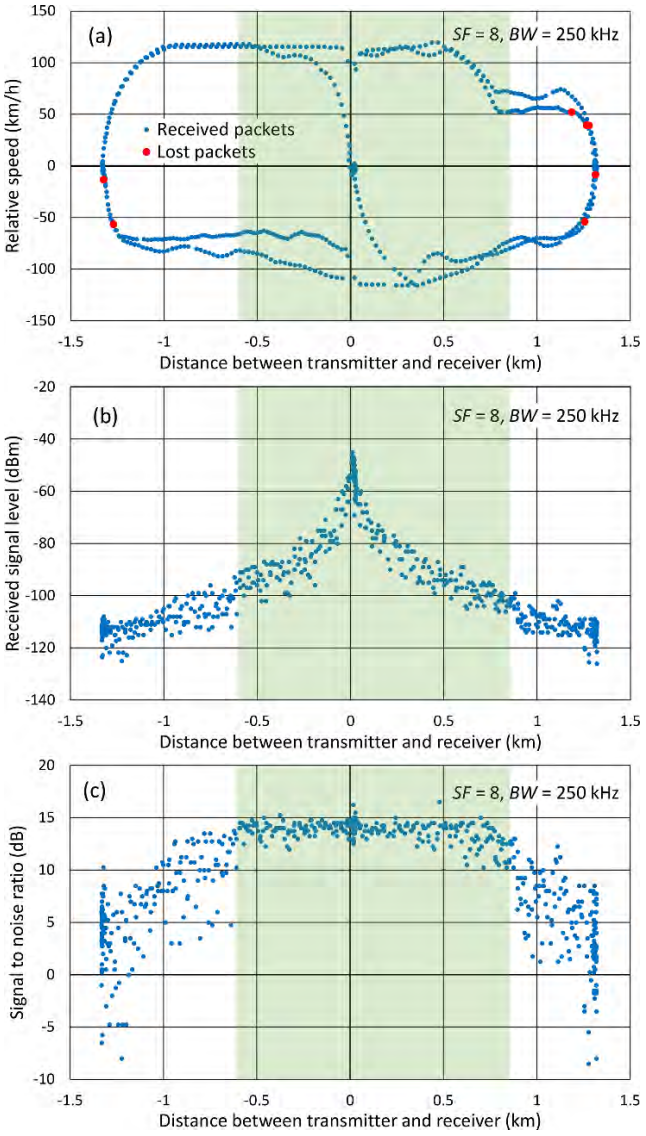


**FIGURE 9.** The results of experiment No. 1 with the LoRa modulation parameters $SF = 8$ and $BW = 250$ kHz: (a) the distribution of received and lost packets in the phase path of the receiver, (b) the signal level at the receiver input, (c) the signal-to-noise ratio at the receiver input. The area in which the line-of-sight conditions are met is highlighted in green.

direction by the terrain relief and in the northwest direction by the forest protection belt after the curve in the highway. It should be noted that the effect of data packets loss due to varying terrain elevation along the trajectory of radio wave propagation was also observed in experiments in which the possibility of using LoRa technology in the Antarctic was investigated [20].

Fig. 10 shows the results of experiment No. 2, performed with the LoRa modulation parameters $SF = 8$ and $BW = 500$ kHz. In total, during experiment No. 2, 958 data packets were transmitted, 27 of which were lost. The sensitivity of the LoRa receiver in this case is 4 dB worse than in experiment No. 1, as a result we lost more packets under the same conditions. As in experiment No. 1, data packets were also lost only when the car with the receiver was out of sight.

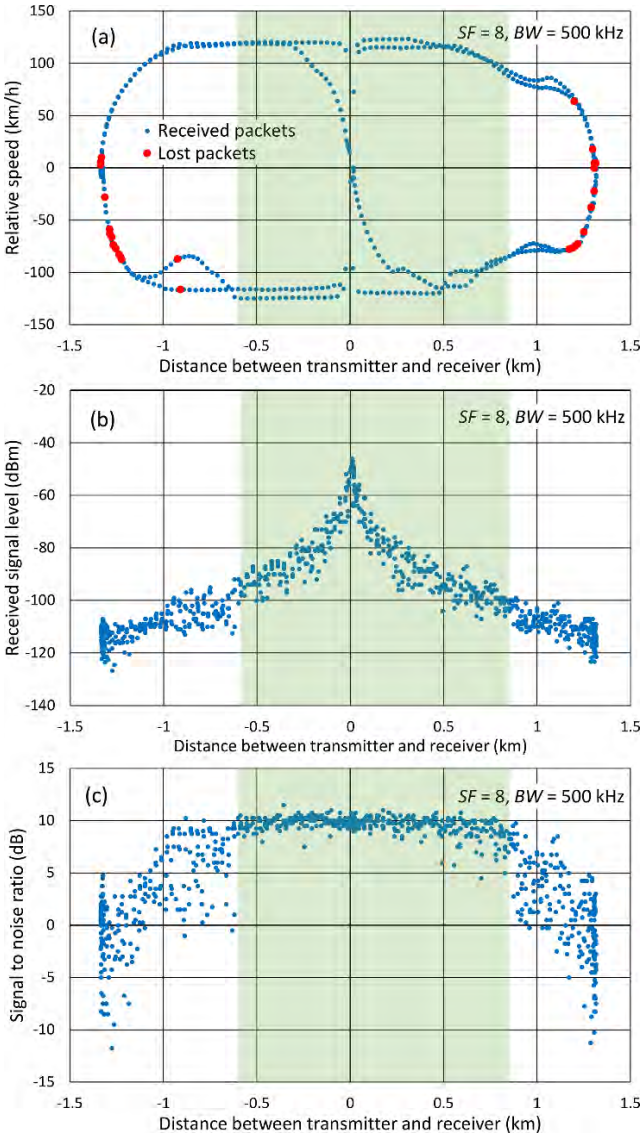


**FIGURE 10.** The same as Fig. 9 but for experiment No. 2 with the LoRa modulation parameters $SF = 8$ and $BW = 500$ kHz.

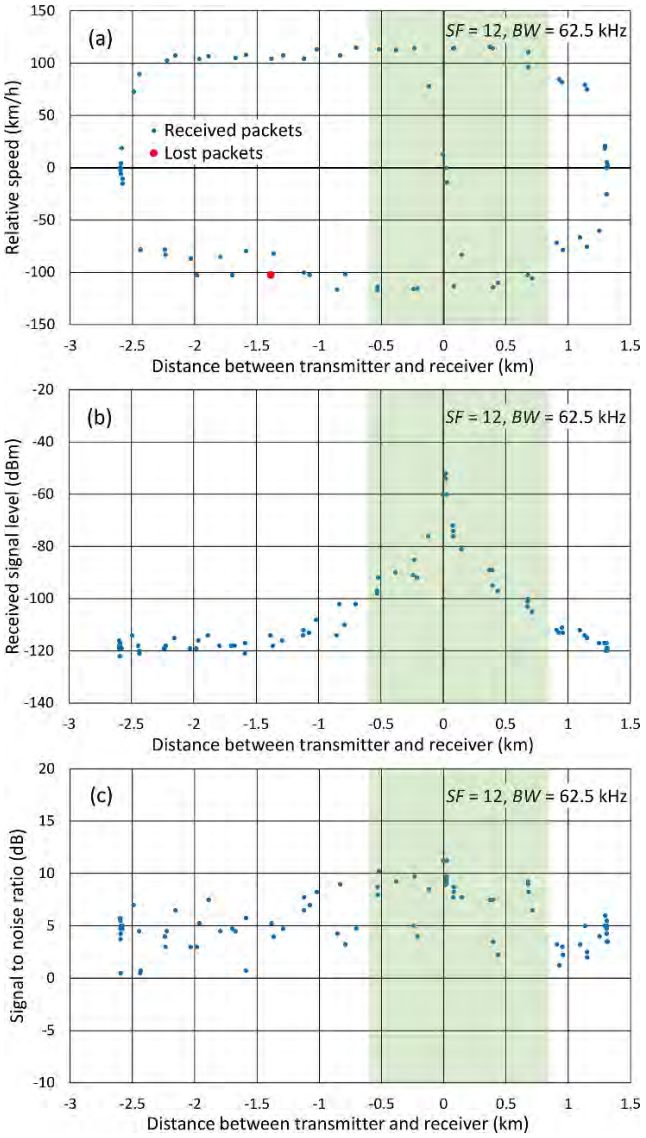


**FIGURE 11.** The same as Fig. 9 but for experiment No. 3 with the LoRa modulation parameters $SF = 12$ and $BW = 62.5$ kHz.

The results of experiment No. 3 performed with the LoRa modulation parameters $SF = 12$ and $BW = 62.5$ kHz are shown in Fig. 11. In this case, the transmission time of a LoRa packet, equal to 2.97 s, is approximately an order of magnitude longer than in previous experiments. Therefore, for the same duration of the experiment, significantly fewer data packets were transmitted. In total, 85 data packets were transmitted during this experiment, only one of which was lost when the car with the receiver was also out of sight. It should be noted that in this case it is difficult to determine the cause of the packet loss, since the signal level at the receiver input did not fall below about $-120$ dBm (see Fig. 11b), which is much higher than the sensitivity of the LoRa receiver in this mode ($-139$ dBm). However, it is important that in this case the loss of the data packet also occurred outside the line-of-sight.

Thus, the outdoor experiments fully confirmed the results of the laboratory experiments, which showed a high robustness of the LoRa modulation against the Doppler effect. In the experiments with a LoRa receiver installed in a car moving in the line of sight of the transmitter, there was not a single case of loss of transmitted data packets at vehicle speeds up to about 120 km/h. This confirms the above conclusion that the deterioration of the LoRa radio communication when the receiver moves in urban conditions with a speed exceeding about 40 km/h, observed in [11], is not the result of the pure Doppler effect, but is the result of the combined influence of multipath propagation and the Doppler effect.

## IV. CONCLUSIONS

We presented here the results of laboratory and outdoor experiments conducted to determine the possibility of using LoRa modulation in radio communication systems of CubeSat nanosatellites in low Earth orbits, as well as to determine possible limitations caused by the strong Doppler effect in these conditions. We investigated the influence of the

Doppler effect on the stability of the LoRa radio channel under various conditions. First, we investigated in the laboratory the static Doppler effect, when the Doppler frequency shift does not change with time. Secondly, we studied the dynamic Doppler effect, when the Doppler frequency shift changes rapidly in time relative to the zero value. In addition, we tested in the laboratory the multipath propagation of the LoRa radio signal and carried out outdoor experiments. These experiments explain the results of experiments with a mobile LoRa receiver, which were conducted in uncontrolled urban environments and demonstrated weak immunity of the LoRa modulation to the Doppler effect.

The laboratory experiments showed a very high resistance of the LoRa modulation to the static Doppler effect for all used values of the spreading factor $SF = 7$, 11, and 12. The LoRa modulation stably operates with a static Doppler shift $\delta F$ up to 55–94.5 ppm, depending on $SF$. These values coincide rather well with the specification of the LoRa SX1278 transceiver [15] regarding the tolerated frequency offset between the transmitter and the receiver for the same modulation modes and the carrier frequency. These maximum allowable Doppler shifts correspond to a receiver speed of about 16.5–28.3 km/s relative to the transmitter, which is several times higher than a satellite speed in a low Earth orbit.

In the case of the dynamic Doppler effect, the specification of the LoRa SX1278 transceiver does not contain any restrictions on the rate of change of Doppler frequency shift $\delta F'$. Our experiments show that the robustness of the LoRa modulation against the dynamic Doppler effect strongly depends on the spreading factor $SF$. With $SF = 7$, the LoRa modulation works stably at $\delta F'$ up to about 150 ppm/s. When $SF$ increases to 11 and 12, the maximum allowable $\delta F'$ value decreases to 4.94 ppm/s and 0.33 ppm/s, respectively.

It is important to note that the maximum allowable values of the Doppler shift and its rate of change, which we obtained for the LoRa radio link, significantly exceed the similar limitations of 25 ppm and 0.275 ppm/s for satellite communications based on quadrature phase shift keying QPSK [21].

Our outdoor experiments with the LoRa receiver installed in a moving car fully confirmed the results of the laboratory experiments, which showed a high robustness of LoRa modulation against the Doppler effect. The outdoor experiments and the laboratory examination of multipath propagation showed that the deterioration of the LoRa communication when the receiver moves in urban conditions with a speed exceeding about 40 km/h, observed in [11], is not the result of the pure Doppler effect, but is the result of the combined influence of multipath propagation and the Doppler effect. In this regard, the results of [11] cannot be applied to the satellite-to-ground radio link, since in this case there is no multipath propagation.

The results obtained are very important for space applications of the LoRa modulation. Our experiments have shown that the LoRa modulation can be used in the radio communication between the ground station and a satellite in a circular orbit more than 550 km in height without any restrictions associated with the Doppler effect. In smaller orbits, the satellite speed increases, with the result that the dynamic Doppler effect becomes an important factor that determines the efficiency of the LoRa modulation. We found that at $SF \leq 11$ there is a significant immunity margin of the LoRa modulation to both the static and dynamic Doppler effect for all orbits, down to the ultra-low Earth orbit with an altitude of 200 km. At $SF = 12$, in orbits less than 550 km in height there is a significant immunity margin of the LoRa modulations only to the static Doppler effect. But the rate of change of the Doppler frequency shift in these orbits exceeds the maximum allowable for $SF = 12$ value of 0.33 ppm/s when the satellite passes directly above the ground station, which means destruction of the LoRa radio communication on this segment of the orbit. This, in turn, means that the dynamic Doppler effect will reduce the communication session between the satellite and the ground station. The maximum reduction in the duration of a communication session of about one minute is expected in an ultra-low orbit 200 km high.

In general, this experimental study confirmed the high immunity of the LoRa modulation to the Doppler effect. This makes it possible to use the LoRa technology in CubeSat radio communication systems and in proposed IoT satellite projects based on the use of satellite constellations in low Earth orbit, including CubeSat constellations. The revealed restriction on the applicability of the LoRa modulation with the spreading factor $SF = 12$ under the conditions of a strong dynamic Doppler effect is very important, but not critical. This means that when planning a satellite LoRa radio channel with $SF = 12$, a more thorough analysis of the communication conditions for a specific satellite orbit is required.

In conclusion, it should be noted that these results obtained in ground-based experiments should be verified using satellite measurements. To this end, we plan to test the results in a real CubeSat experiment in the near future.

## APPENDIX

### GLOSSARY OF ACRONYMS

| | |
|---|---|
| BW | Band Width |
| CSS | Chirp Spread Spectrum |
| FSK | Frequency Shift Keying |
| GLONASS | Global Navigation Satellite System |
| GPS | Global Positioning System |
| IoT | Internet of Things |
| LEO | Low Earth Orbit |
| QPSK | Quadrature Phase Shift Keying |
| RF | Radio Frequency |
| SDR | Software-Defined Radio |
| SF | Spreading Factor |
| USB | Universal Serial Bus |

## ACKNOWLEDGMENT

The authors thank Anatoly Pelemeshko and Oleg Bragin for their help in performing outdoor experiments, and Samuel Peana for manuscript preparation assistance.

## REFERENCES


[1] C. A. Hornbuckle, "Fractional-N synthesized chirp generator," U.S. Patent 7 791 415 B2, Sep. 7, 2010.

[2] C. Goursaud and J. M. Gorce, "Dedicated networks for IoT: PHY/MAC state of the art and challenges," *EAI Endorsed Trans. Internet Things*, vol. 15, no. 1, Oct. 2015, Art. no. e3.

[3] A. Augustin, J. Yi, T. Clausen, and W. M. Townsley, "A study of LoRa: Long range & low power networks for the Internet of Things," *Sensors*, vol. 16, no. 9, Sep. 2016, Art. no. 1466.

[4] LoRa, Semtech Corporation, Camarillo, CA, USA. (May 2015). *Modulation Basics, Application Note AN1200.22, Rev. 2*. [Online]. Available: https://www.semtech.com/uploads/documents/an1200.22.pdf

[5] L. Vangelista, "Frequency shift chirp modulation: The LoRa modulation," *IEEE Signal Process. Lett.*, vol. 24, no. 12, pp. 1818–1821, Dec. 2017.

[6] D. Selva and D. Krejci, "A survey and assessment of the capabilities of cubesats for earth observation," *Acta Astronaut.*, vol. 74, pp. 50–68, May/Jun. 2012.

[7] F. Davoli, C. Kourogiorgas, M. Marchese, A. Panagopoulos, and F. Patrone, "Small satellites and cubesats: Survey of structures, architectures, and protocols," *Int. J. Satell. Commun. Netw.*, vol. 37, no. 4, pp. 343–359, Jul./Aug. 2019. Accessed: Sep. 4, 2018. [Online]. Available: https://onlinelibrary.wiley.com/doi/10.1002/sat.1277. doi: 10.1002/sat.1277.

[8] Z. Qu, G. Zhang, H. Cao, and J. Xie, "Leo satellite constellation for Internet of Things," *IEEE Access*, vol. 5, pp. 18391–18401, 2017.

[9] Y. Qian, L. Ma, and X. Liang, "Symmetry chirp spread spectrum modulation used in LEO satellite Internet of Things," *IEEE Commun. Lett.*, vol. 22, no. 11, pp. 2230–2233, Nov. 2018.

[10] I. F. Akyildiz and A. Kak, "The Internet of space things/cubesats: A ubiquitous cyber-physical system for the connected world," *Comput. Netw.*, vol. 150, pp. 134–149, Feb. 2019.

[11] J. Petäjäjärvi, K. Mikhaylov, M. Pettissalo, J. Janhunen, and J. Iinatti, "Performance of a low-power wide-area network based on LoRa technology: Doppler robustness, scalability, and coverage," *Int. J. Distrib. Sensor Netw.*, vol. 13, no. 3, pp. 1–16, Mar. 2017. doi: 10.1177/1550147717699412.

[12] D. Patel and M. Won, "Experimental study on low power wide area networks (LPWAN) for mobile Internet of Things," in *Proc. IEEE 85th Veh. Technol. Conf. (VTC Spring)*, Jun. 2017, pp. 1–5. doi: 10.1109/VTCSpring.2017.8108501.

[13] J. C. Liando, A. Gamage, A. W. Tengourtius, and M. Li, "Known and unknown facts of LoRa: Experiences from a large-scale measurement study," *ACM Trans. Sensor Netw.*, vol. 15, no. 2, Mar. 2019, Art. no. 16.

[14] A. Doroshkin, A. Zadorozhny, O. Kus, V. Prokopyev, and Y. Prokopyev, "Laboratory testing of LoRa modulation for cubesat radio communications," in *Proc. MATEC Web Conf.*, vol. 158, Mar. 2018, Art. no. 01008.

[15] Semtech Corporation, Camarillo, CA, USA. (Jan. 2019). *SX1276/77/78/79—137 MHz to 1020 MHz Low Power Long Range Transceiver, Datasheet, Rev. 6*. [Online]. Available: https://www.semtech.com/uploads/documents/DS_SX1276-7-8-9_W_APP_V6.pdf

[16] National Instruments, Austin, TX, USA. (Jan. 2011). *NI PXIe-5672 Specifications. RF Vector Signal Generator*. [Online]. Available: http://www.ni.com/pdf/manuals/372342d.pdf

[17] D. King-Hele, *Satellite Orbits in an Atmosphere: Theory and Applications*. Glasgow, U.K.: Blackie, 1987.

[18] T. S. Rappaport, *Wireless Communications: Principles and Practice*, 2nd ed. Upper Saddle River, NJ, USA: Prentice-Hall, 2001.

[19] Raspberry PI Foundation, Cambridge, U.K.*Raspberry Pi 2 Model B. Specifications*. [Online]. Available: https://www.raspberrypi.org/products/raspberry-pi-2-model-b/

[20] J. Gaelens, P. Van Torre, J. Verhaevert, and H. Rogier, "LoRa mobile-to-base-station channel characterization in the Antarctic," *Sensors*, vol. 17, no. 8, Aug. 2017, Art. no. 1903.

[21] L. Ouvry, D. Lachartre, C. Bernier, F. Lepin, F. Dehmas, and V. Deslandes, "An ultra-low-power 4.7mA-Rx 22.4mA-Tx transceiver circuit in 65-nm CMOS for M2M satellite communications," *IEEE Trans. Circuits Syst., II, Exp. Briefs*, vol. 65, no. 5, pp. 592–596, May 2018.


**ALEXANDER A. DOROSHKIN** graduated in radio physics from the Physics Department, Novosibirsk State University, Russia, in 1990.

He is currently an Assistant Professor with the Department of General Physics, Novosibirsk State University, where he is also a Lead Engineer with the Division for Atmospheric Research. His research interests include electronics engineering, wireless communication and communications for the satellite-based Internet of Things, industrial automation, rocket, and satellite experiments.

**ALEXANDER M. ZADOROZHNY** graduated in radio physics from the Physics Department, Novosibirsk State University, Russia, in 1971, and received the Ph.D. degree in atmospheric physics from Novosibirsk State University, in 1982.

He is currently the Head of the Division for Atmospheric Research, Novosibirsk State University, where he is also an Associate Professor with the Department of General Physics. His research interests involve composition and electrodynamics of the middle atmosphere, Earth's ozone layer, noctilucent clouds, external influences on the middle atmosphere, and rocket and satellite experiments.

Dr. Zadorozhny is a member of the American Geophysical Union and an Associate of the Committee on Space Research.

**OLEG N. KUS** graduated in computations and networks from the Department of Automation and Computational Systems, Novosibirsk State Technical University, Russia, in 1996.

He is currently a Founder and a CEO of the OKB Fifth Generation Ltd., Novosibirsk, Russia. His research interests include electronics engineering, wireless communication, and the satellite-based Internet of Things.

**VITALIY YU. PROKOPYEV** graduated in quantum electronics from the Physics Department, Novosibirsk State University, Russia, in 2004.

He is currently the Head of the Laboratory of Small Satellites, Novosibirsk State University, where he is also an Assistant Professor with the Department of General Physics His research interests include electronics engineering in space instrumentation, embedded programming, and small satellite design.

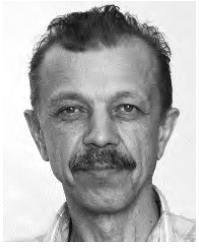

**YURI M. PROKOPYEV** graduated in radio physics from the Physics Department, Novosibirsk State University, Russia, in 1981, and received the Ph.D. degree in technical sciences from Novosibirsk State University, in 1995.

He is currently the Head of the Laboratory of Space Experiments, Novosibirsk State University, where he is also an Associate Professor with the Department of General Physics. His research interests include space instrumentation, space experiments and the influence of space factors on a spacecraft.